https://doi.org/10.17221/85/2020-VETMED

Autologous adipose-derived mesenchymal stem cells and hydroxyapatite for bone defect in rabbits

Guilherme Galhardo Franco[1], Bruno Watanabe Minto[1], Livia de Paula Coelho[1], Patricia Furtado Malard[2], Elizabeth Regina Carvalho[1], Fernando Yoiti Kitamura Kawamoto[1], Brenda Mendonca de Alcantara[1], Luis Gustavo Gosuen Goncalves Dias[1]*

[1]*Department of Clinical and Veterinary Surgery, Faculty of Agrarian and Veterinary Sciences, São Paulo State University (UNESP), Jaboticabal, SP – Brazil*
[2]*BioCell, Brasília, DF – Brazil*

**Corresponding author: brealcantara@yahoo.com.br*

Citation: Franco GG, Minto BW, Coelho LP, Malard PF, Carvalho ER, Kawamoto FYK, Alcantara BM, Dias LGGG (2022): Autologous adipose-derived mesenchymal stem cells and hydroxyapatite for bone defect in rabbits. Vet Med-Czech 67, 38–45.

Abstract: This study aims to evaluate the effect of autologous adipose-derived mesenchymal stem cells (AAD-MSC), with and without synthetic absorbable hydroxyapatite (HAP-91), on the bone regeneration in rabbits. Thirty-four female white New Zealand rabbits were submitted to a 10 mm distal diaphyseal radius ostectomy, divided into 3 experimental groups according to the treatment established. The bone gap was filled with 0.15 ml of a 0.9% saline solution containing two million AAD-MSC (G1), or AAD-MSC associated with HAP-91 (G2). The control group (CG) received only 0.15 ml of the 0.9% saline solution. Radiographs were made post-operatively, and after 15, 30, 45 and 90 days. Fifty percent of the samples were submitted to a histological examination at 45 days and the remaining ones at 90 days post-operatively. Radiographically, the periosteal reaction, bone callus volume and bone bridge quality were superior in G2 ($P < 0.05$). Histologically, the bone repair was faster and more efficient in G1 at 45 days ($P < 0.05$). In conclusion, AAD-MSC improved the regeneration on the experimentally induced bone defects in rabbits; however, the use of hydroxyapatite requires caution given the granulomatous reaction produced in the species.

Keywords: adipose derived MSC; cell transplantation; fracture healing; *Oryctolagus cuniculus*

An appropriate intervention is crucial to potentiate the physiological repair mechanisms in bone fractures, particularly when there is a critical failure or bone integration is expected to be challenging, such as substantial bone loss due to trauma or tumour resection, non-union or delayed union, arthroplasties, and patients with systemic comorbidities (Ho-Shui-Ling et al. 2018).

Innovations and improvements involving biomaterials and cellular therapy used for fracture management have been used to optimise bone unions (Venkatesan et al. 2016). Following this reality, mesenchymal stem cells (MSC) have emerged as important aids in veterinary medicine (Voga et al. 2020). These cells are easily isolated and grown in cultures, show multipotentiality, immunomodulatory and paracrine effects, besides their migration capacity (Naji et al. 2019).

According to tissue engineering concepts, many tissues and organs can be regenerated using MSC sown in three-dimensional scaffolds (Li et al. 2019). The study conducted by de Girolamo et al. (2011) demonstrated that a hydroxyapatite disk seeded with rabbit autologous adipose-derived mesen-

https://doi.org/10.17221/85/2020-VETMED

chymal stem cells (AAD-MSC) can be a promising treatment for critical bone defects. However, more clinical trials are needed to evaluate the usefulness of these cells in veterinary orthopaedics. The aim of this study was to investigate the use of AAD-MSC, with and without synthetic absorbable hydroxyapatite (HAP-91), in the bone regeneration in rabbits.

MATERIAL AND METHODS

Animals and experimental design

All the procedures described below were in compliance with the institutional Animal Care and Use Committee (Protocol No. 007168/15).

Thirty-four female white New Zealand rabbits (*Oryctolagus cuniculus*), 160–170 days old, 3.5–4.5 kg, were included in the experiment and randomly divided into three groups (G1: n = 13; G2: n = 10; CG: n = 11), according to the treatment established.

Mesenchymal stem cells harvesting

The G1 and G2 animals were premedicated with morphine (2 mg/kg), midazolam (2 mg/kg), and ketamine (25 mg/kg) (intramuscularly, i.m.). The anaesthetic induction and maintenance were undertaken with isoflurane in 100% oxygen, through a face mask.

Initially, 10 g to 25 g of adipose tissue was harvested from the fatty sac in the interscapular area and stored for 2 min in a tube with 50 ml of a sterile cell washing solution. It was conditioned in a second washing tube for three minutes, and placed in a third tube containing the transport medium.

At the laboratory, the samples were washed three times with a phosphate buffered saline (PBS; Reprodux, Itapira, SP, Brazil), chopped into small pieces and placed in contact with a collagenase 0.075% concentration in PBS with a low Ca and Mg and hyaluronidase 0.1% (1 mg/ml) solution so that enzymatic digestion could be carried out. For the digestion, the tissue that was in contact with the digestive solution was incubated at 37 °C for 40 min, being homogenised every 5 minutes. The enzymatic inactivation was performed with PBS supplemented with 10% Faetal Bovine Serum (FBS; GIBCO, Big Cabin, OK, USA). The mixture was centrifuged at 290 × g for 10 min and the cell button was washed in 5 ml of Dulbecco's modified eagle medium (DMEM; Sigma-Aldrich, St. Louis, MO, USA) with 10% FBS, the washed cells were centrifuged at 290 × g for 5 minutes. The washing process was repeated three times. Then, the cell viability was analysed using the trypan blue percent counting method.

After being isolated, MSC were grown in T25 culture flasks with DMEM supplemented with 10% FBS and incubated in a humid environment at 37 °C and in a 5% CO_2 atmosphere. The cell culture medium was changed every 2 days until 80% confluence was reached. Once the desired confluence was reached, the cells were trypsinised and transferred to T75 culture bottles. Again, the culture medium was changed every 2 days until 80% confluence was reached. Then the cells were trypsinised and frozen in straws, at a concentration of one million cells per straw. The cells were cryopreserved using a cell freezing medium composed of 80% DMEM, 10% dimethyl sulfoxide (DMSO; Sigma-Aldrich, St Louis, MO, USA) and 10% FBS, and kept frozen in liquid nitrogen until use.

As a standard procedure for the quality control of the mesenchymal stem cell culture, a sample of the cells was induced to differentiate into the bone tissue using a StemPro® Osteogenesis Differentiation Kit (Invitrogen, Waltham, MA, USA) in a 12-well plate, with a half change every two days for approximately 25 days. After differentiation, the plate was stained with Alizarin Red (Sigma Aldrich, St Louis, MO, USA) to detect the bone matrix through calcium red staining. The cells were characterised by flow cytometry with image quantification and identification of the molecular markers. Molecular characterisation tests for the MSC were performed as determined by the International Society for Cell Therapy (Dominici et al. 2006). The surface markers positive for the tested MSCs were mouse anti-human CD29-RD1 (Beckman Counter, Brea, CA, USA), mouse anti-equine CD44-FITC (AbD Serotec, Raleigh, NC, USA), caprine anti-canine CD90 primary (Washington State University, Pullman, WA, USA) and mouse IgM anti-caprine conjugated AF594 (secondary) (Thermo Fisher Scientific, Waltham, MA, USA). The negative surface marker for the tested MSCs was mouse anti-human CD34-FITC (Invitrogen, Waltham, MA, USA). These markers

https://doi.org/10.17221/85/2020-VETMED

were evaluated by the immunophenotyping method on an Amnis® Imaging Flow Cytometer (Luminex, Austin, TX, USA). The MSC showed high capacity for adhesion to plastic, phenotypic characteristics typical of MSC and were attached to the bottom of the bottle with a fusiform shape when reaching 80% confluence. The results of the immunophenotyping showed that 90% of the cells expressed the three surface undifferentiation markers CD29, CD44 and CD90 and had low expression of the negative marker CD34. Still, 96% showed expression of the pluripotency transcription factor SOX2 and 92% of OCT3/4.

Surgical induction of segmental bone defect

Using the same anaesthetic protocol, a 2.5 cm craniomedial skin incision was made at the end of the right radius and a 10 mm long ostectomy was made in the radial diaphysis, 15 mm above the radiocarpal joint, using an oscillatory saw, in all the animals.

In group 1 (G1), two million of AAD-MSC resuspended in 0.15 ml of a 0.9% sterile saline solution was applied percutaneously into the bone defect. In group 2 (G2), the defect was filled with HAP-91® (JHS Biomateriais, Sabará, MG, Brazil) followed by the MSC application in the same way. In the control group (CG), 0.15 ml of the 0.9% sterile saline solution was injected percutaneously. The muscular and subcutaneous tissue were closed with a continuous pattern, and the skin was closed with a simple interrupted suture, using 4.0 nylon.

Clinical evaluation

The animals were observed daily, and the surgical wound was checked for oedema or secretions on the 3rd and 7th post-operative days, when palpation of the affected limb was performed to identify pain and a lameness observation was also undertaken. Scores were attributed to these parameters according to Table 1.

Radiographic evaluation

Radiographs were made in mediolateral and craniocaudal projections (mA = 100, KV = 40 and mAs = 3.2), immediately post-operatively and after 15, 30, 45 and 90 days.

Their evaluations were double-blinded made by three different evaluators. The periosteal reaction, bone callus formation, and bone bridge quality between fragments were the semi-quantitative parameters measured, based on An et al. (1999) and Ozturk et al. (2008).

Histological evaluation

Randomly, at 45 days, 50% of the animals in each group (16 animals) were euthanised and the remaining animals were euthanised at 90 days post-operatively.

The radius and ulna were fixed in formaldehyde for 48 h and decalcified in 7% nitric, daily, for approximately 2 to 3 days. These were embedded in paraffin and cut into a 5 mm microtome, and sequentially stained with haematoxylin and eosin and Masson trichrome.

Under optic microscopy, the neovascularisation, inflammatory infiltrate, formation of fibrous tissue, formation of cartilaginous tissue, formation of bone tissue, quality of the union and formation of a bone bridge were quantified using scores (Table 1). The bone architecture and morphology of the new bone formation were described.

Statistical analysis

The statistical analyses were performed using a commercially available statistical software (Prism Windows v5.0; GraphPad Software, CA, USA). The Shapiro-Wilk test was used to investigate the normal distribution of the data.

Comparisons between the groups and times were accomplished by the Kruskal-Wallis test, due to the non-parametric data. The statistical significance was defined as $P \leq 0.05$.

Table 1. Scale for the semi-quantititative evaluation of the clinical and histological parameters

Score	Characteristic of the parameter
1	absent
2	mild
3	moderate
4	severe

https://doi.org/10.17221/85/2020-VETMED

RESULTS

Regarding the clinical evaluation, the lowest mean score for the pain on palpation (1.6) and for the lameness (3.1) of the affected limb was seen in G1 on the 3rd day post-operatively, although this difference was not statistically significant ($P > 0.05$).

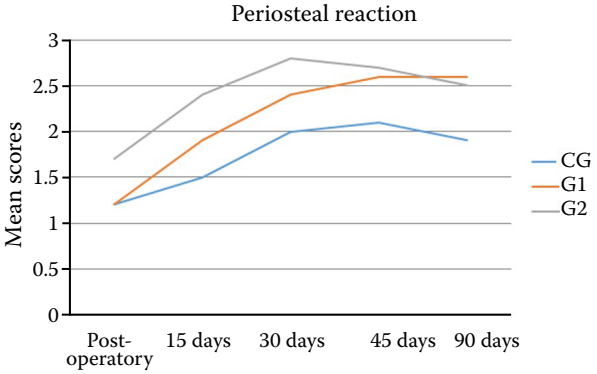

Figure 1. Development of the mean scores of the radiographic evaluations of the periosteal reaction in all the groups

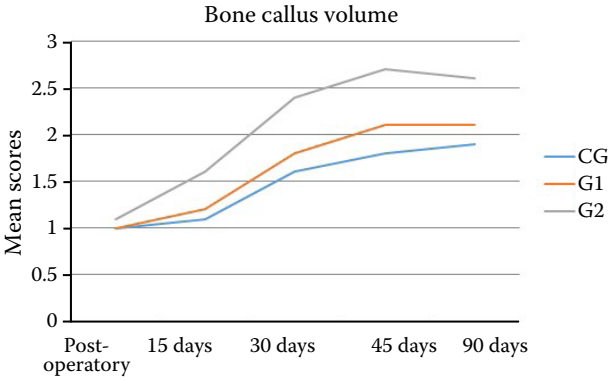

Figure 2. Development of the mean scores of the radiographic evaluation of the bone callus volume in all the groups

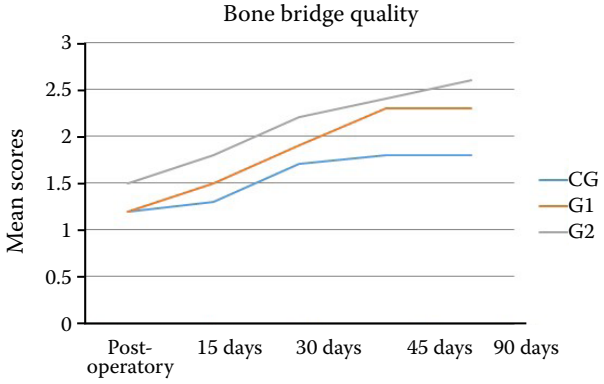

Figure 3. Development of the mean scores of the radiographic evaluation of the bone bridge quality in all the groups

At this moment, the lowest oedema score (1.7) ($P < 0.05$) was recorded in G1, against 2.7 and 2.5 in CG and G2, respectively.

By the 7th day, all the animals were using the affected limb.

About the radiographic evaluation, the periosteal reaction was more evident in G2 at 15, 30 and 45 days. At 90 days, the periosteal reaction in G2 was similar to G1 and superior to CG ($P < 0.05$) (Figure 1). The bone callus volume was higher in G2 in all of the evaluation time points (Figure 2) and from 30 days, it was higher in G1 than in CG ($P < 0.05$). Considering the bone bridge quality, G2 was superior to G1 and G1 was superior to CG at all the evaluation moments (Figures 3–6).

In the histopathological analysis, at 45 days, 75% of the animals in CG had no bone bridge, and the bone defect was predominantly filled by fibrous or fibrocartilaginous tissues. Moreover, mild neovascularisation was present in the bone defect region, and there was no inflammatory infiltrate. At 90 days, 80% of the animals in CG showed non-union, the bone defect was filled with fibrocartilaginous tissue and the medullary canal was thin and closed (Figure 7A). Only 22% of the rabbits from CG showed bone healing.

At 45 days, 100% of the rabbits in G1 showed bone healing and a bone bridge with an intense formation of the periosteal trabecular bone, and

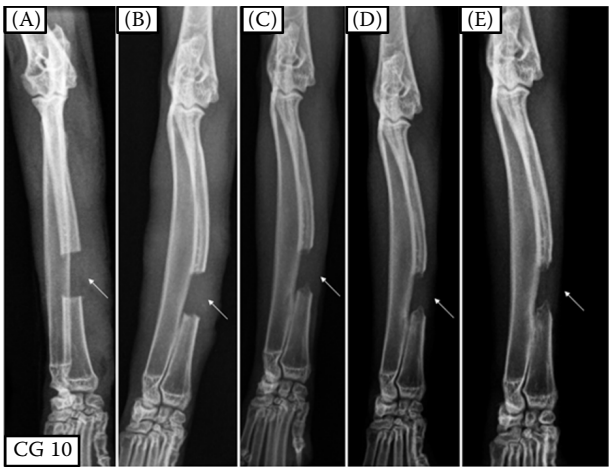

Figure 4. Radiographic images in the craniocaudal projection of the bone reparation process in animal number 10 of the control group (CG)

(A) Immediate post-operatory, the segmental bone defect at the distal diaphysis of radius (arrow). (B) 15 days post-operatively. (C) 30 days post-operatively. (D) 45 days post-operatively. (E) 90 days post-operatively. The repair process was insufficient, resulting in a non-union

https://doi.org/10.17221/85/2020-VETMED

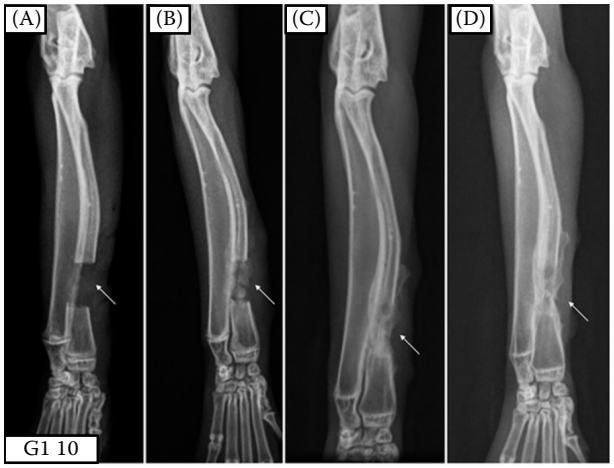

Figure 5. Radiographic images in the craniocaudal projection of the bone healing process in animal number 10 of the mesenchymal stem cells group (G1)
(A) Radiography at immediately post-operatively of the segmental defect (arrow). (B) 15 days post-operatively, intense periosteal reaction at the segmental defect at the distal diaphysis of the radius (arrow). (C) 30 days post-operatively, the bone callus completely filled the bone defect (arrow). (D) 45 days post-operatively, the defect completely filled by a bone callus (arrow). Note the intense periosteal reaction at the extremity of the radius, adjacent to the bone defect

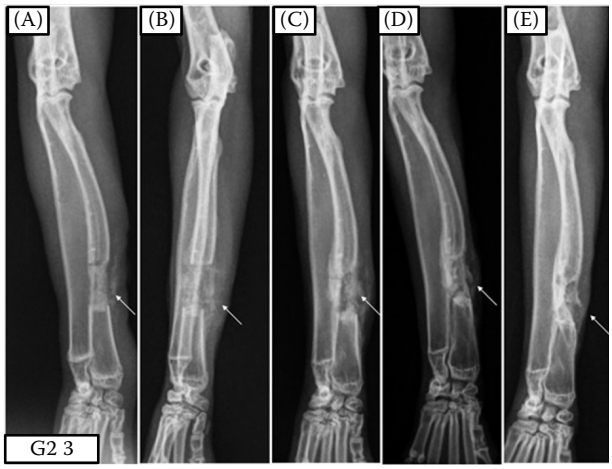

Figure 6. Radiographic images in the craniocaudal projection of the bone healing process in animal number 3 of the mesenchymal stem cells and hydroxyapatite group (G2)
(A) Radiography immediately post-operatively of the segmental defect at the distal diaphysis of the radius filled with hydroxyapatite (arrow). (B) 15 days post-operatively, moderate periosteal reaction (arrow). (C) 30 days post-operatively, intense periosteal reaction (arrow). (D) 45 days post-operatively, intense periosteal reaction and initial remodelling (arrow). (E) 90 days post-operatively, the bone defect is filled by a bone callus (arrow)

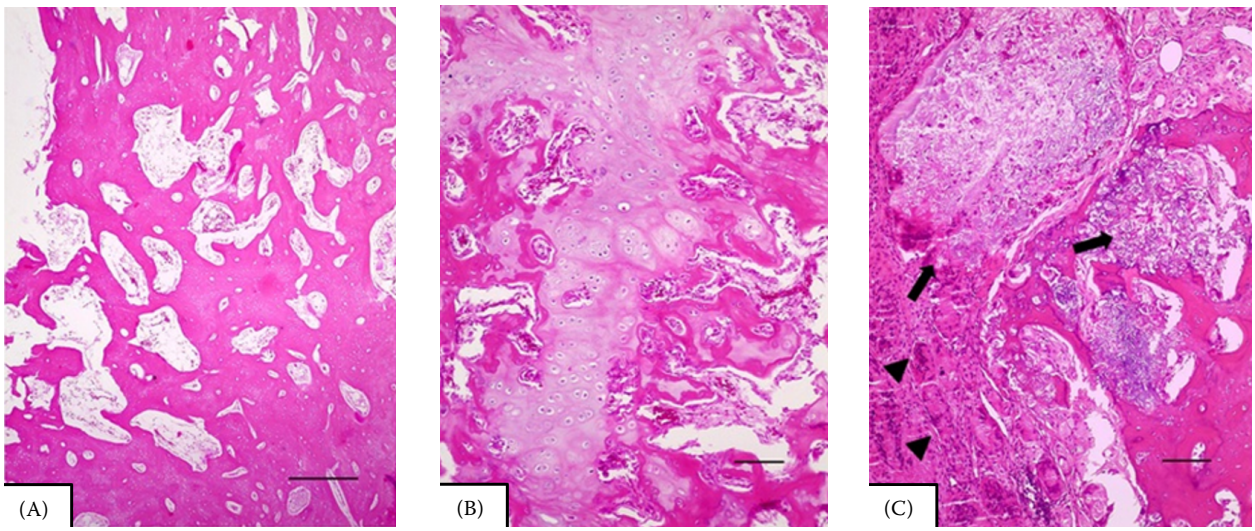

Figure 7. Histological analysis of the bone segmental defect at the distal diaphysis of radius on a rabbit of each group, at 90 days
(A) Control group: Prominent bone proliferation and complete non-union [haematoxylin and eosin (H&E), 400 μm]. (B) G1: Detail of the cartilaginous and bone formation (H&E, 400 μm). (C) G2: Hydroxyapatite deposits (arrow) surrounded by an intense granulomatous inflammation containing multinucleated giant cells (H&E, 100 μm)

reestablishment of the cortex. At 90 days, 71.4% of the rabbits in G1 had maximum scores on the histological evaluation of the bone bridge and union quality (Figure 7B). The neovascularisation was discrete, and there was no inflammatory infiltrate in any animal.

https://doi.org/10.17221/85/2020-VETMED

In G2, 60% of animals had maximum scores on the histological evaluation of the bone bridge and union quality at 45 days, and 100% at 90 days. A periosteal and endosteal intense granulomatous inflammation and HAP-91 deposits surrounded by giant cells were present (Figure 7C). The fibrous tissue formation was moderate to intense in all the animals from G2, and was statistically significantly superior to that in CG or G1 ($P < 0.05$).

The treated animals showed better healing of the bone defect in comparison with that in CG. Although the animals in G2 had higher medium scores for the bone tissue formation at 45 and 90 days than those in the other groups ($P < 0.05$), the animals in G1 exhibited a better and more effective bone bridge formation and better quality of the union at 45 days ($P < 0.05$). The G1 animals showed intense formation of the periosteal trabecular bone tissue, decreased cartilaginous tissue and better structural and morphological organisation at 45 days than the G2 animals.

DISCUSSION

Many studies have demonstrated promising results for improvements in bone healing using cellular therapy associated with biomaterials (Tajima et al. 2015; Venkatesan et al. 2016; Volkov et al. 2020). Our results provide strong evidence of the beneficial effects of MSC in bone neoformation in segmental defects in the distal radial diaphysis. The radiographic and histological evaluations indicate that the action of MSC, alone or associated with HAP-91, allowed 31% of the G1 rabbits and 20% of the G2 animals to complete bone healing, in a critical size defect. Moreover, the rabbits in the G1 and G2 that failed to show complete healing, still had a periosteal reaction and trabecular bone formation clearly superior than those in CG.

Radiographically, the healing in G2 was superior, while the histological healing parameters of the bone tissue formation, bone bridge formation and quality of the union were better in G1 at 45 days. Additionally, G1 showed faster bone healing in comparison to G2, in which there was a high score of fibrous tissue formation interspersed with bone tissue. The radiographic evaluation of G2 was difficult due to the radiopacity of the hydroxyapatite, which made it difficult to differentiate the pellets from the periosteal reaction or a bone callus, particularly in the initial evaluations, so the radiographic scores may have been overestimated in this group.

Synthetic hydroxyapatite is a plastic biomaterial that acts like a scaffold to the neovascularisation, cellular proliferation, fibrovascular growth, osteoid formation and growth of mineralised bone (Pereira-Junior et al. 2013). It has osteoconductive properties (Ramesh et al. 2018), and can be combined with MSC to promote osteogenic induction (Chi et al. 2020). In this study, hydroxyapatite showed the characteristics of a good scaffold, promoting an intense periosteal reaction in association with AAD-MSC. Nevertheless, the rabbits in G2 developed an intense inflammatory infiltrate, with foamy macrophages and giant cells developing around the hydroxyapatite deposits, impairing the bone healing process. Rabbits have a high tendency towards excessive granulation tissue against foreign materials, which could explain the reaction seen in our study (Rich 2002).

G1 showed the lowest score of all the groups for the post-operative oedema, probably due to the anti-inflammatory effects of MSC. PGE2, one of the mainly soluble factors secreted by MSC, is a central mediator of the immunomodulatory response over other immune cells. Among its actions, it has antiproliferative effects on T lymphocytes and NKs (natural killer cells), and modulates the release of inflammatory substances from dendritic cells and macrophages (Martinet et al. 2009). However, we hypothesise that the oedema reduction was not seen in G2 due to granulomatous reaction induced by HAP-91.

One study described the beneficial effects of adipose-derived MSC on the neovascularisation of skin lesions, secondary to the secretion of angiogenic cytokines [vascular endothelial growth factor (VEGF) and hepatocyte growth factor (HGF)] (Nauta et al. 2013). Moreover, many studies report the formation of vessels promoted by VEGF during bone healing and remodelling (Stegen et al. 2015). In spite of the potential benefits, there was no statistical difference in the neovascularisation between the groups. It is possible that the histological analysis was not able to quantify the neovascularisation due to the low density of blood vessels and discreet coverage of soft tissues on the distal radial diaphysis. Immunohistochemistry would be a more appropriate method for this purpose.

In this study, the used AAD-MSCs were isolated from the adipose tissue of each animal in a prior

https://doi.org/10.17221/85/2020-VETMED

procedure, featuring an autologous cell therapy; however heterologous MSCs have been used in veterinary practice as they are rapidly available, in a fast and safe way, and can be stored in a cell bank frozen in liquid nitrogen. The MSCs express major class I histocompatibility complex (MHC I) molecules, but do not express class II histocompatibility complexes (MHC II), thus, they are unable to produce alloreactivity in mammals (Aggarwal and Pittenger 2005), which is important because it prevents the cell's rejection.

A limitation of the present study was the species included, since clinically, the target species are dogs, cats and even humans.

Meanwhile, the rabbit is a widely used experimental animal model for the study of bone pathophysiology and bone healing processes (Pearce et al. 2007).

Further studies are necessary to elucidate the actions of MSC, especially about the stimuli that lead to their differentiation, which could allow the better use of these cells in tissue regeneration.

In conclusion, the use of AAD-MSC is beneficial to bone healing in critical size segmental bone defects in the distal radial diaphysis in rabbits. The association of MSC with HAP-91 produced an intense granulomatous reaction in this species that delayed the healing process, although G2 was the only group where there were no cases of non-union and more homogeneous results were observed between the animals.

Conflict of interest

The authors declare no conflict of interest.

REFERENCES

Aggarwal S, Pittenger MF. Human mesenchymal stem cells modulate allogeneic immune cell responses. Blood. 2005 Feb 15;105(4):1815-22.

An YH, Friedman RJ, Draughn RA. Animal models of bone fracture or osteotomy. In: An YH, Friedman RJ, editors. Animal models in orthopaedic research. Boca Raton: CRC Press; 1999. p. 197-217.

Chi H, Chen G, He Y, Chen G, Tu H, Liu X, Yan J, Wang X. 3D-HA scaffold functionalized by extracellular matrix of stem cells protomotes bone repair. Int J Nanomedicine. 2020 Aug 6;15:5825-38.

de Girolamo L, Arrigoni E, Stanco D, Lopa S, Di Giancamillo A, Addis A, Borgonovo S, Dellavia C, Domeneghini C, Brini AT. Role of autologous rabbit adipose-derived stem cells in the early phases of the repairing process of critical bone defects. J Orthop Res. 2011 Jan;29(1):100-8.

Dominici M, Le Blanc K, Mueller I, Slaper-Cortenbach I, Marini FC, Krause DS, Deans RJ, Keating A, Prockop DJ, Horwitz EM. Minimal criteria for defining multipotent mesenchymal stromal cells. The International Society for Cellular Therapy position statement. Cytotherapy. 2006 Jan 1;8(4):315-7.

Ho-Shui-Ling A, Bolander J, Rustom LE, Johnson AW, Luyten FP, Picart C. Bone regeneration strategies: Engineered scaffolds, bioactive molecules and stem cells current stage and future perspectives. Biomaterials. 2018 Oct; 180:143-62.

Li H, Shen S, Fu H, Wang Z, Li X, Sui X, Yuan M, Liu S, Wang G, Guo Q. Immunomodulatory functions of mesenchymal stem cells in tissue engineering. Stem Cells Int. 2019 Jan 13;2019:1-18.

Martinet L, Fleury-Cappellesso S, Gadelorge M, Dietrich G, Bourin P, Fournie JJ, Poupot R. A regulatory cross-talk between Vγ9Vδ2 T lymphocytes and mesenchymal stem cells. Eur J Immunol. 2009 Mar;39(3):752-62.

Naji A, Eitoku M, Favier B, Deschaseaux F, Rouas-Freiss N, Suganuma N. Biological functions of mesenchymal stem cells and clinical implications. Cell Mol Life Sci. 2019 Sep;76(17):3323-48.

Nauta A, Seidel C, Deveza L, Montoro D, Grova M, Ko SH, Hyun J, Gurtner GC, Longaker MT, Yang F. Adipose-derived stromal cells overexpressing vascular endothelial growth factor accelerate mouse excisional wound healing. Mol Ther. 2013 Feb;21(2):445-55.

Ozturk A, Ilman AA, Saglam H, Yalcinkaya U, Aykut S, Akgoz S, Ozkan Y, Yanik K, Kivcak B, Yalcin N, Ozdemir RM. The effects of phytoestrogens on fracture healing: Experimental research in New Zealand white rabbits. Ulus Travma Acil Cerrahi Derg. 2008 Jan;14(1):21-7.

Pearce AI, Richards RG, Milz S, Schneider E, Pearce SG. Animal models for implant biomaterial research in bone: A review. Eur Cell Mater. 2007 Mar 2;13:1-10.

Pereira-Junior OCM, Rahal SC, Lima-Neto JF, Landim-Alvarenga FC, Monteiro FOB. In vitro evaluation of three different biomaterials as scaffolds for canine mesenchymal stem cells. Acta Cir Bras. 2013 May;28(5):353-60.

Ramesh N, Moratti SC, Dias GJ. Hydroxyapatite-polymer biocomposites for bone regeneration: A review of current trends. J Biomed Mater Res B Appl Biomater. 2018 Jul;106(5):2046-57.

Rich GA. Rabbit orthopedic surgery. Vet Clin North Am Exot Anim Pract. 2002 Jan 1;5(1):157-68.

https://doi.org/10.17221/85/2020-VETMED

Stegen S, van Gastel N, Carmeliet G. Bringing new life to damaged bone: The importance of angiogenesis in bone repair and regeneration. Bone. 2015 Jan;70:19-27.

Tajima S, Tobita M, Orbay H, Hyakusoku H, Mizuno H. Direct and indirect effects of a combination of adipose-derived stem cells and platelet-rich plasma on bone regeneration. Tissue Eng Part A. 2015 Mar;21(5-6):895-905.

Venkatesan J, Lowe B, Anil S, Kim SK, Shim MS. Combination of nano-hydro xyapatite with stem cells for bone tissue engineering. J Nanosci Nanotechno. 2016 Sep;16(9): 8881-94.

Voga M, Adamic N, Vengust M, Majdic G. Stem cells in veterinary medicine – Current state and treatment options. Front Vet Sci. 2020 May 29;7:1-20.

Volkov AV, Muraev AA, Zharkova II, Voinova VV, Akoulina EA, Zhuikov VA, Khaydapova DD, Chesnokova DV, Menshikh KA, Dundun AA, Makhina TK, Bonartseva GA, Asfarov TF, Stamboliev IA, Gazhva YV, Ryabova VM, Zlatev LH, Ivanov SY, Bonartsev AP. Poly(3-hydroxybutyrate)/hydroxyapatite/alginate scaffolds seeded with mesenchymal stem cells enhance the regeneration of critical-sized bone defect. Mater Sci Eng C. 2020 Sep; 114:1-14.

Received: April 9, 2020
Accepted: August 2, 2021